The structure of liquid methanol: a molecular dynamics study using a six-site model

1999 J. Phys.: Condens. Matter 11 9151

(http://iopscience.iop.org/0953-8984/11/47/303)

J. Phys.: Condens. Matter **11** (1999) 9151–9163. Printed in the UK PII: S0953-8984(99)06782-X

The structure of liquid methanol: a molecular dynamics study using a six-site model

L Bianchi†, A K Adya†§, O N Kalugin†‖ and C J Wormald‡

† School of Science and Engineering, Division of Molecular and Life Sciences, University of Abertay-Dundee, Bell Street, Dundee DD1 1HG, UK
‡ School of Chemistry, University of Bristol, Cantocks Close, Bristol BS8 1TS, UK

E-mail: a.adya@tay.ac.uk

Received 9 August 1999

Abstract. Molecular dynamics (MD) simulations of pure methanol (216 molecules) have been carried out at 298.15 K in the NVE ensemble using a six-site potential model originally derived by Anwander *et al* (1992 *Chem. Phys.* **166** 341) from *ab initio* quantum chemical calculations (QCC) and tested for the first time in this study. MD results of a three-site model where all the methyl hydrogens were considered as a dead load have also been reported recently by us. In this paper, the relative merits of the two models are discussed by comparing the simulated radial distribution functions (rdfs) with the recent experimental neutron diffraction (ND) results obtained at the partial pair distribution function (pdf) level. Although the MD simulations with both the models reproduce the total rdfs rather well, discrepancies begin to appear at the partial pdf level. Both the simulations are found to reproduce equally well the X–X (X = C, O or H, a methyl hydrogen) pdf since it comprises six correlations, and is dominated mainly by contributions from the methyl group. However, the main peaks of the simulated H_O–H_O partial, where H_O is the hydroxyl hydrogen, are found to be slightly higher and shifted to larger distances as compared to the ND results. A comparison of the simulated X–H_O intermolecular rdf, in which H–H_O correlations dominate, with the ND results shows that, although the three-site model reproduces at least qualitatively the experimental features, the six-site model derived from *ab initio* QCC fails badly.

1. Introduction

Since the pioneering computer simulations on liquid methanol performed by Jorgensen [1], many potential models have been parametrized to reproduce various structural and dynamical properties of this liquid [2–11]. Two classes of models can be distinguished: the three-site models [2–4, 6, 11] in which usually the carbon atom along with the three methyl hydrogens is treated as a unified interaction site and the six-site models where all the atoms are explicitly considered [5, 7, 9, 10]. By using these different potential models conflicting conclusions [3, 11–13] have been made about the favoured structure of liquid methanol which is governed mainly by its hydrogen-bonding interactions. Recently, neutron diffraction (ND) structural results on liquid methanol [14, 15] have been reported at the pdf level by performing H/D isotopic substitution on hydroxyl hydrogen, H_O. A comparison of the simulated structural results with those derived experimentally at the pdf level can help in discriminating against spurious models. In a previous paper [16] we tested a widely used three-site potential model

§ Corresponding author.
‖ Permanent address: Department of Inorganic Chemistry, Kharkov State University, Kharkov, Svobody Square 4, 310077, Ukraine.

0953-8984/99/479151+13$30.00

Table 1. Molecular geometry, moments of inertia and dipole moment of the methanol molecule.

Parameter	Experimental [19]	Experimental [18]	H1 + CH_3 [6]	APR6 [17]	*Ab initio* MP2/TZV (2p, 2d)++ QCC
d_{OH_O} (Å)	0.937	0.9451 ± 0.0034	0.9451	0.956	0.958 25
d_{CO} (Å)	1.434	1.4246 ± 0.0024	1.4246	1.427	1.4286
d_{CH_i} (Å)	—	1.0936 ± 0.0032	1.0936	1.096	1.0838 ($i = 3$)
					1.0893 ($i = 1, 2$)
$\angle COH_O$ (°)	105.93	108.53 ± 0.48	108.53	108.9	107.60
$\angle OCH_i$ (°)	—	—	—	106.6 ($i = 3$)	106.5 ($i = 3$)
				111.6 ($i = 1, 2$)	111.8 ($i = 1, 2$)
$\angle H_iCH_j$ (°)	109.5	108.63 ± 0.70	108.63	109.0	108.68 ($i = 1, 2$; $j = 3$)
					109.21 ($i = 1$; $j = 2$)
$\angle\tau$ (°)	—	3.27 ± 0.18	3.27	—	—
$\tau(H_OOCH_3)$	—	—	180.0	180.0	180.0
I_A (amu Å^2)	3.961	3.96277	3.9178	3.9596	3.92
I_B (amu Å^2)	20.533	20.4834	20.4780	20.5332	20.5130
I_C (amu Å^2)	21.283	21.2679	21.2147	21.2828	21.2548
q_{H_O} (e)	—	—	0.431	0.338	0.313[a]
q_O (e)	—	—	−0.728	−0.549	−0.492[a]
q_C (e)	—	—	0.297	−0.104	−0.171[a]
q_{H_i} (e)	—	—	0.0	0.105	0.11 ($i = 1, 2$)
					0.130 ($i = 3$)
$\mu_\parallel$ (D)	−0.885	—	—	—	−1.029[b]
$\mu_\perp$ (D)	1.44	—	—	—	1.487[b]
μ (D)	1.69	—	2.33	2.08	1.88[a] (1.81)[b]
$\angle\vec{\mu}, \vec{O}H_O$ (°)	50.6	—	55.8	65.3	66.4

[a] From the Mulliken population analyses.
[b] Dipole moments calculated directly from molecular orbital MP2/TZV (2p, 2d)++ wavefunctions.

(H1) devised by Haughney *et al* [6] against our ND structural results. Although this model could satisfactorily reproduce the rdfs at the total level, discrepancies occurred at the partial pdf level. In this paper we report molecular dynamics (MD) simulations of pure methanol (216 molecules) using a six-site potential (hereafter referred to as the APR6 model) parametrized by Anwander *et al* [17]. The computational procedure used in the MD simulations is described in section 2. In section 3 we compare the simulated structural results using the APR6 (six-site) model with those obtained with the extended H1 (three-site) model in which the methyl hydrogens were treated as a dead load. The relative merits of using the six- or three-site model are discussed in section 4. These results are discussed by comparing the simulated results with our recent neutron diffraction (ND) results [14]. The conclusions are summarized in the last section.

2. Computational procedure

Each methanol molecule (see figure 1) has been treated as a rigid object consisting of six sites corresponding to the oxygen (O), the carbon (C), the hydrogen of the hydroxyl group (H_O) and methyl hydrogens (H_1, H_2, H_3). The bond lengths d_{OH_O}, d_{CO}, d_{CH_i} ($i = 1, 2, 3$), $\angle OCH_i$, $\angle COH_O$, $\angle H_iCH_j$ and torsional angle, $\tau(H_OCH_i)$ were taken from [17] (reference 42 therein), and are listed in table 1. The calculated moments of inertia along the three principal axes,

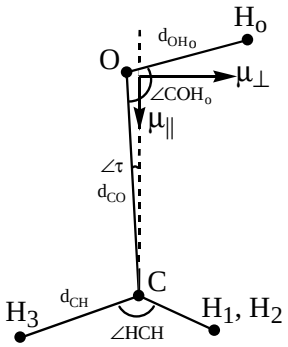

Figure 1. The molecular geometry of the methanol molecule used for the MD simulations with the H1 + CH_3 model and the APR6 model in which H_3, C, O and H_O lie in the symmetry plane of the molecule.

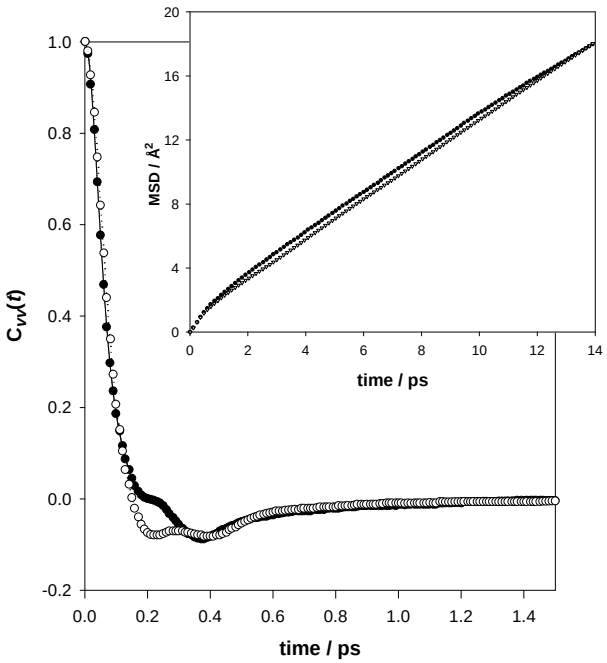

Figure 2. Normalized centre-of-mass (c.o.m.) velocity auto-correlation functions (VACFs), $C_{vv}(t)$, obtained for the H1 + CH_3 model (●) and the APR6 model (○). Also shown in the inset is the c.o.m. mean square displacement for the H1 + CH_3 model (●) and the APR6 model (▽).

I_A, I_B, I_C, are also listed together with the experimental values [18, 19]. In our previous MD simulation [16] using the extended H1 model, we used the intramolecular parameters from Lees and Baker [18]. The geometric parameters of the two models are in good agreement with each other and also with those obtained by *ab initio* quantum chemical calculations (QCC) at the second order Møller-Plesset level (MP2) with the TZV(2p, 2d)++ basis set performed by using the GAMESS programme package [20] reported in this paper. These geometric models are found not to produce any perceivable difference in the intramolecular structure.

Table 2. Liquid methanol properties from MD simulations using two different force fields.

	APR6	H1 + CH_3	Experiment
Long-range (Coulomb) Interaction treatment	EW	EW	—
Ensemble	NVE	NVE	—
Algorithm	FIQA rigid body	FIQA rigid body	—
Equilibration time (ps)	80	70	—
Sampling time (ps)	100	100	—
$\langle T \rangle$ (K)	293.6 ± 8.9	301.1 ± 9.2	Ambient temperature
$-\langle U \rangle_{corr}$ (kJ mol^{-1})[a]	[b]	35.3 ± 0.2	34.95[c]
$-\langle U \rangle_{uncorr}$ (kJ mol^{-1})[a]	18.5 ± 0.2	31.42 ± 0.2	
$\langle P \rangle_{corr}$ (kbar)[a]	[b]	0.85 ± 0.39	Ambient pressure
$\langle P \rangle_{uncorr}$ (kbar)[a]	6.6 ± 0.28	1.04 ± 0.39	
$D \times 10^9$ (m^2 s^{-1})[d]	1.94 (2.05)	2.01 (1.92)	2.42^{e}_{5}

[a] corr/uncorr stand for values corrected/uncorrected for the potential truncation.
[b] A proper estimation of these values cannot be made (see text).
[c] Experimental potential energy was calculated from the measured [25] enthalpy of vaporization at 298.15 K.
[d] Values outside parenthesis obtained from the centre-of-mass (c.o.m.) velocity auto-correlation function (VACF) while those within were obtained using the c.o.m. mean square displacement (MSD).
[e] Taken from [27].
EW and FIQA stand for Ewald summation and Fincham's implicit quaternion algorithm.

Any differences in the structure of liquid methanol produced by different potential models (to be discussed in section 3) can thus be assigned to the different force fields employed in the simulations, and do not result from the different geometric models.

The six-site potential model, APR6, used in these simulations was parametrized from an *ab initio* study of the interaction energy hypersurface for the methanol dimer by Anwander *et al* [17]. The pair potential was derived from the fit of 332 calculated CEP-31G**/HF dimer energies using a polynomial expression,

$$V_{ij}(r_{ij}) = A_{ij}/r_{ij}^{l} + B_{ij}/r_{ij}^{m} + C_{ij}/r_{ij}^{n} + q_i q_j/4\pi\varepsilon_0 r_{ij} \qquad \text{with } l > m > n. \tag{1}$$

O, C, H_O, and methyl hydrogens (H) are the interaction sites, A_{ij}, B_{ij} and C_{ij} are the fitted parameters between sites i and j of distinct molecules, the l, m, n are the exponents, q_i is the partial charge on site i and r_{ij} is the site–site separation (all given in [17]). Since the results of the APR6 simulation will be compared with those of our previous MD simulation using the extended H1 model, we give here a brief account of this model. A fuller account of the model is given elsewhere [6, 16]. H1 is a potential model semi-empirically parametrized to reproduce basic macroscopic properties of liquid methanol. Each methanol molecule is considered as a rigid body with three interacting sites corresponding to oxygen (O), the methyl group (C) treated as united atom and hydrogen of the hydroxyl group (H_O). The pair intermolecular potential is the sum of Lennard-Jones (LJ) and Coulomb parts,

$$V_{ij}(r_{ij}) = \frac{q_i q_j}{4\pi\varepsilon_0 r_{ij}} + 4\varepsilon_{ij}[(\sigma_{ij}/r_{ij})^{12} - (\sigma_{ij}/r_{ij})^{6}] \tag{2}$$

where ε_{ij} and σ_{ij} are the LJ parameters between sites i and j of distinct molecules, q_i is the partial charge on site i and r_{ij} is the site–site separation. In our recent MD simulations [16] three hydrogens of the methyl group were explicitly taken into account as dead load and this extended model was denoted as H1 + CH_3. It is interesting to note (see table 1) that the

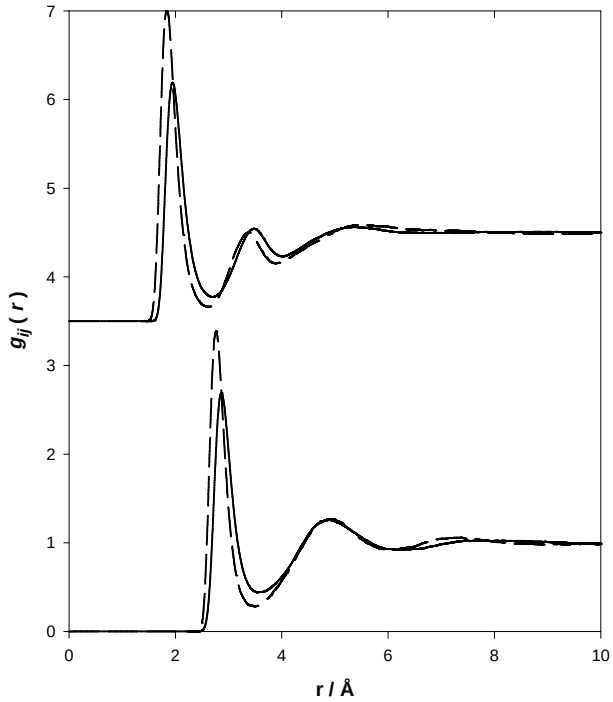

Figure 3. O–H_O (top, displaced by +3.5) pdf obtained from the MD simulations with the APR6 (solid line) and H1 + CH_3 (dashed line) models. Comparison of O–O pdf (bottom) obtained with the APR6 (solid line) and the H1 + CH_3 (dashed line) models.

H1 + CH_3 model gives values that are closer to the experimental values for the angle between the dipole moment vector and the OH_O bond direction, $\angle\bar{\mu}$, $O\bar{H}_O$ of the methanol molecule than those given by APR6 or MP2/TZV(2p, 2d)++ QCC. However, since experimental data of dipole moments for liquids have large uncertainties, which depend on the theory used in the data treatment [21, 22], only qualitative comparison can be made. Table 1 shows that APR6 and MP2/TZV(2p, 2d)++ QCC give a better representation of electrostatic interactions since both produce a dipole moment (2.08 D and 1.88 D, respectively) in better agreement with the experimental gas phase value of 1.69 D than the H1 + CH_3 model (2.33 D). The larger value of the dipole moment in the H1 + CH_3 model was used [6] in order to take approximate account of induction forces in the liquid phase. In the APR6 model however, the dipole–dipole and charge-induced-dipole interactions are taken into account by a large number of terms with exponents $n = 3$.

The equations of motion were integrated using the Verlet leap-frog algorithm for translational motion of the centre-of-mass of the methanol molecules, and the Fincham's implicit quaternion algorithm [23] (FIQA) for rotational motion of rigid bodies. The MD simulations were performed using the DL_POLY_2.0 MD simulation package [24] in the NVE ensemble at 298.15 K with 216 methanol molecules placed in a cubic box with periodic boundary conditions. The box length of 24.45 Å was chosen so as to match the experimental density, at 298.15 K, of 0.786 37 g cm^{-3} [25]. A cut-off radius equal to half the box length was applied to all interactions. In all MD runs, the time step was equal to 0.002 ps. Ewald summation [26] (EW) was used for handling the long-range Coulombic interactions. Table 2 summarizes the details of MD simulations performed by using the APR6 and H1+CH_3 (for comparison) models.

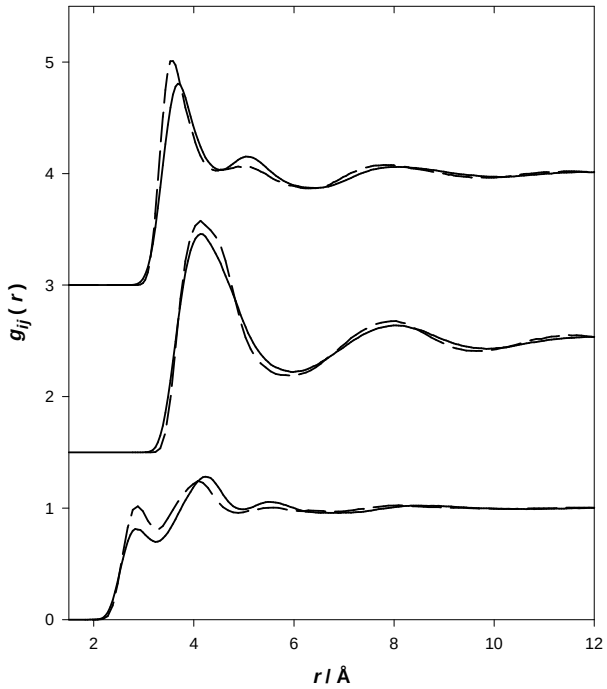

Figure 4. H_O–C (bottom), C–C (middle, displaced by +1.5) and O–C (top, displaced by +3) pdfs (dashed lines: the H1 + CH_3 model, solid lines: the APR6 model).

The presence of inverse cubic terms in the APR6 model does not allow us to calculate the potential truncations to the configurational energy and pressure using standard treatments [28]. As a result, exact comparison of thermodynamic properties obtained from the simulation by using the APR6 model with the corresponding experimental values cannot be made (table 2). Nevertheless, since the system temperatures obtained by using the two models are found to be in agreement with each other within the amplitude of the statistical fluctuations, it is possible to compare the single particle dynamics obtained from the two models.

For both the simulations, the diffusion coefficients were obtained for hydrogenated methanol by using the centre-of-mass (c.o.m.) mean square displacements (MSDs) via the Einstein relation [28], and by integrating the velocity auto-correlation functions (VACFs) via the Green–Kubo relation [28]. These show (see table 2) reasonable agreement with each other and also with the experimental value. Figure 2 compares the evolution of the MSD and the normalized VACFs, $C_{vv}(t)$,

$$C_{vv}(t) = \langle \boldsymbol{v}(t)\boldsymbol{v}(0)\rangle / \langle \boldsymbol{v}(0)^2\rangle \tag{3}$$

from the two models. While the MSDs are similar, one can clearly see differences in the two VACFs. The appearance of a negative correlation region with its minimum at about 0.4 ps for MD simulations performed with both the models can be interpreted as being due to the 'rebound' of the tagged molecule against the cage formed by its nearest neighbours. The first minimum at $\sim$0.2 ps is much emphasized in the APR6 relative to that in the H1 + CH_3 model. To what extent this feature may be associated with relaxation processes occurring with different lifetimes cannot be ascertained from the present studies, since the analysis is only based on translational motion of the centre-of-mass.

3. Partial distribution functions

The partial pair distribution functions (pdfs) (except H_O–H_O, which will be discussed in detail in section 4.2) obtained from the APR6 simulation are plotted together with those obtained using the H1 + CH_3 model in figures 3–5. It is worth noting that while the APR6 potential was parametrized using the gas phase energy hypersurface obtained from *ab initio* QCC of methanol dimers, the H1 + CH_3 model was devised especially for the liquid state [6, 29]. Figures 3–5 show that there is reasonable agreement between the APR6 and H1 + CH_3 generated pdfs. This suggests that the APR6 model potential obtained from first principles is transferable to the liquid phase of methanol, as was also inferred earlier (see section 2) from the good agreement of the two diffusion coefficient values. Co-ordination numbers as well as positions of extrema of the pdfs are compared with the experimental results in table 3.

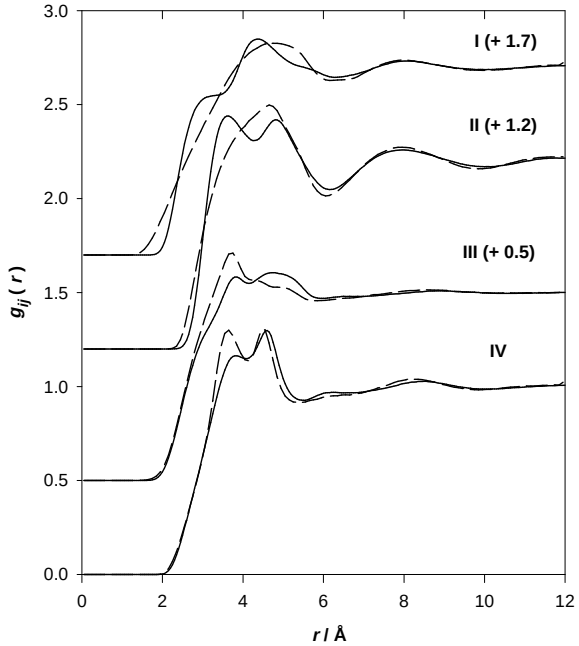

Figure 5. H–H (I), C–H (II), H_O–H (III) and O–H (IV) pair distribution functions (dashed lines: the H1 + CH_3 model; solid lines: the APR6 model). These correlations have been obtained by averaging over the three methyl hydrogens: H1, H_2 and H_3.

It can be seen from figure 3 and table 3 that the main peaks of the O–H_O and O–O simulated partials obtained with the APR6 model are smaller and are shifted towards higher distances compared to those obtained with the H1 + CH_3 model. This may suggest that there are fewer H-bonded molecules for the liquid simulated by the APR6 model. The most pronounced differences, as expected, are seen (figure 5) in the case of H–H, C–H, H_O–H and O–H pdfs. Indeed, since in the APR6 the methyl hydrogens are treated as interaction sites, the simulated partials obtained from this model show more structure than those from the H1 + CH_3 model in which the methyl hydrogens were used merely as a dead load. As a result, the H1 + CH_3 model has a tendency to average out (see, e.g. H–H and C–H pdfs in figure 5) the structural features exhibited by the APR6. Thus, the two peaks in the C–H pdf at 3.65 Å and 4.8 Å in the APR6 model have become a broad single peak in the H1 + CH_3 model.

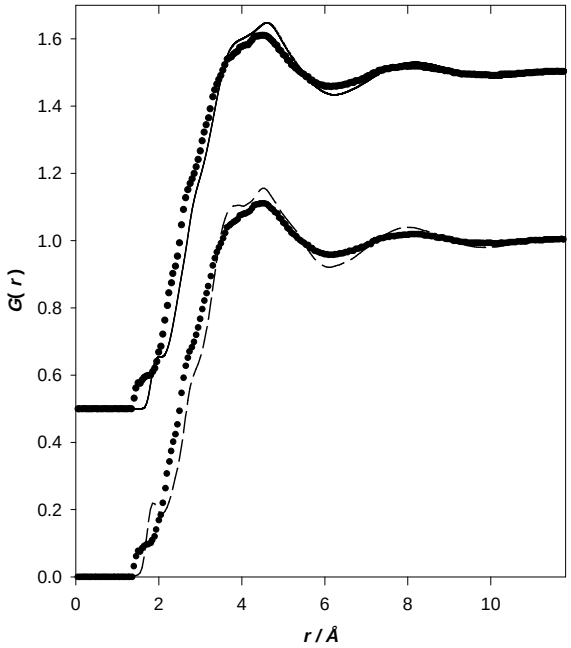

Figure 6. Intermolecular radial distribution function for CD_3OD obtained from MD simulation with the H1+CH_3 model (dashed line) and the APR6 model (solid line displaced by +0.5) compared to the ND results (symbols).

Table 3. Characteristics of the pdfs, $g_{ij}(r)$ in liquid methanol obtained with the H1 + CH_3 and the APR6 (values in parenthesis) models compared with the available experimental data.

pdf	r_{M1} (experimental) (Å)	r_{M1} (Å)	r_{m1} (Å)	$g(r_{M1})$	r_{M2} (Å)	$n(r_{m1})$	$n(r)$ (experimental)
O–O	2.76–2.80[a],	2.79 (2.88)	3.53 (3.58)	3.38 (2.68)	4.93 (4.88)	2.07 (2.09)	
	2.66 [b], 2.798[c]					1.87 (1.71)	1.8[c]
O–C	3.8[d]	3.60 (3.68)	4.48 (4.53)	2.01 (1.8)	5.10 (5.03)	5.00 (5.04)	
O–H_O	1.75 ± 0.03[e]	1.88 (1.93)	2.63 (2.68)	3.47 (2.7)	3.38 (3.48)	0.98 (0.96)	
O–H	—	3.65 (3.85)	4.10 (4.10)	1.30 (1.16)	4.50 (4.60)	1.94 (1.81)	
H_O–H_O	2.4[f],2.36[e]	2.49 (2.58)	3.38 (3.53)	2.79 (2.64)	— —	2.32 (2.70)	2.8[g]
H_O–C	—	2.83 (2.83)	3.28 (3.23)	1.01 (0.81)	4.08 (4.23)	1.13 (0.90)	
H_O–H	—	3.70 (3.85)	5.85 (4.15)	1.21 (1.08)	— (4.75)	6.80 (1.93)	
C–C	3.8 and 4.4[d,h]	4.18 (4.13)	5.90 (5.99)	2.07 (1.96)	8.00 (8.04)	12.3 (12.9)	
C–H	—	4.65 (3.65)	6.05 (4.25)	1.30 (1.24)	7.90 (4.80)	7.60 (2.10)	
H–H	—	4.85 (4.40)	6.20 (6.30)	1.13 (1.15)	7.95 (8.10)	5.77 (6.00)	

[a] [30].
[b] From crystalline data [31].
[c] [32].
[d] [33].
[e] [14].
[f] [34].
[g] Calculated up to $r = 3.37$ Å which is the minimum after the first peak.
[h] 3.8 and 4.4 Å correspond to two distinct C–C contributions.
r_{M_i} is the position of the ith maximum, r_{m1} the position of the first minimum, $g(r_{M1})$ the height of the first maximum and n the co-ordination number.

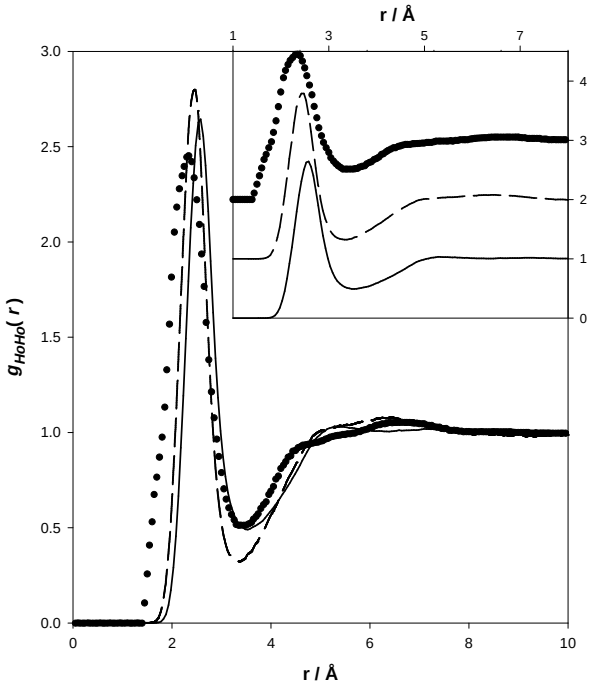

Figure 7. H_O–H_O partial distribution function for methanol obtained from MD simulation with the H1 + CH_3 model (dashed line) and the APR6 model (solid line) compared to the one obtained experimentally (symbols). Inset: APR6 model (bottom), H1 + CH_3 model (middle, displaced by +1) and experimental (top, displaced by +2).

4. Comparison with the neutron diffraction results

4.1. Total intermolecular rdfs

The 21 partial pdfs obtained by the APR6 MD simulations (figures 3–5) have been combined in the ratio of their relative neutron weights, $W_{\alpha\beta}$ (listed in [14]) to reconstruct the total intermolecular rdf for deuterated methanol. Figure 6 shows that the total rdfs from both APR6 and H1+CH_3 models reproduce satisfactorily the neutron diffraction results reported elsewhere [14]. Although the rdfs from both simulations are somewhat shifted towards higher distances at low r, it is worth noticing that even the shoulder observed experimentally at 2.8 Å is well reproduced by the simulations. At higher distances, although the periodicity of the oscillations is in agreement with the ND results, ND data smear out more rapidly. From a comparison of the two model potentials, it can be seen that although they are fundamentally different, both of them reproduce equally well the structure of liquid methanol at the total rdf level. This underlines the fact that no critical validation of any potential model can be done at the total rdf level.

4.2. Partial rdfs

ND isotopic (H/D) substitution (NDIS) on the hydroxyl hydrogen of methanol was used [14] recently to extract the H_O–H_O, X–H_O and X–X partials, where X are the non-substituted species. In the following section we discuss results obtained from MD simulation with these ND results.

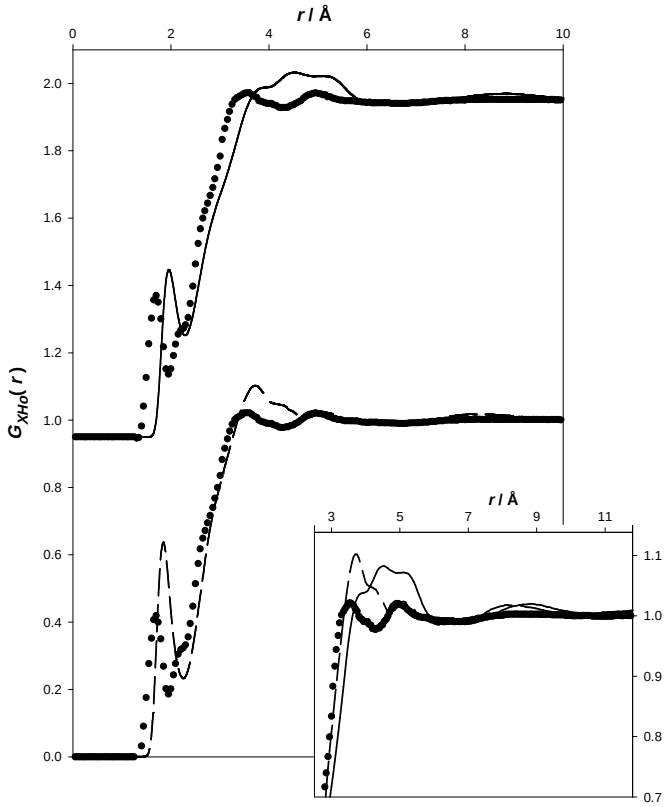

Figure 8. Intermolecular X–H_O partial distribution functions obtained from MD simulation with the H1 + CH_3 model (dashed line) and the APR6 model (solid line displaced by +0.95) compared to the one obtained experimentally (symbols). The same functions are overlaid on a different scale in the inset.

A comparison of the H_O–H_O pdf obtained from both simulations (APR6 and H1 + CH_3) with the one obtained from NDIS shows good agreement (see figure 7). However, it can be seen that relative to the experimental rdf there is an overall shift towards higher distances in the simulated rdfs. For instance, the main peak maxima (also see table 3) of the MD simulations are shifted towards higher distances ($\sim$0.13 Å for H1 + CH_3 and $\sim$0.22 Å for APR6) as compared to the ND results. In addition, the minimum distance of closest approach and the rdf at low r-values from the two simulations is found to be significantly different from the experimental results. It may be that the model potentials used in both simulations underestimate the closest approach of the two H_O atoms.

The H/D substitution on the H_O makes it possible to look at the correlations of this atom with its closest neighbours through the intermolecular $G^{\text{inter}}_{XH_O}(r)$ distribution function. This function is now reduced to a weighted sum of only three pdfs (C–H_O, O–H_O and H–H_O),

$$G^{\text{inter}}_{XH_O}(r) = \sum_{X \neq H_O} W_{XH_O} g_{XH_O}(r) \qquad \text{where X} = \text{C, H and O.} \tag{4}$$

The relative weights of the C–H_O, O–H_O and H–H_O partials are about 0.20, 0.18 and 0.61, respectively. The MD equivalent functions constructed for both the force field models, along with the one derived from NDIS, are presented in figure 8. Reference to figures 3–5 reveals that firstly, the main correlation contributing to the first peak in $G^{\text{inter}}_{XH_O}(r)$ is the O–H_O and

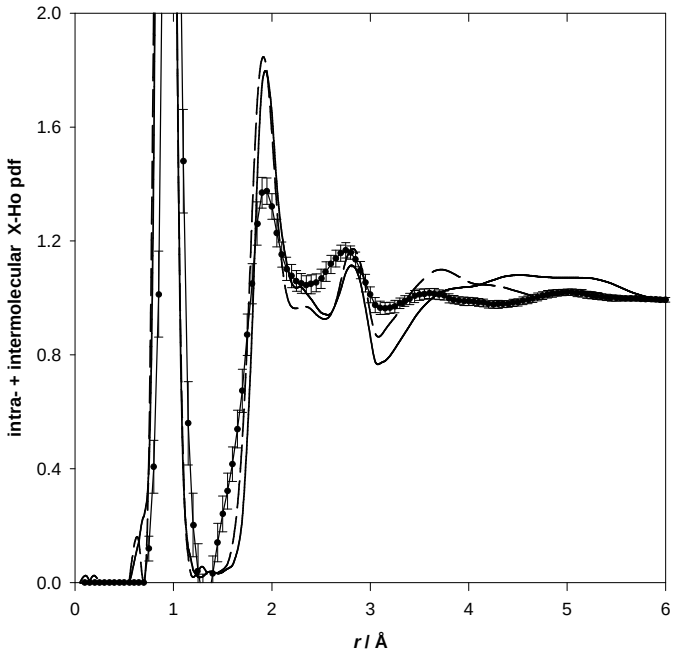

Figure 9. Intra- + intermolecular X–H_O partial distribution functions obtained from MD simulations with the H1 + CH_3 model (dashed line) and the APR6 model (solid line), reconstructed according to the used geometrical model of methanol, as compared to the one obtained experimentally (symbols with error bars).

secondly, although the two models agree with each other to within experimental error, they fail to reproduce the ND peak at a quantitative level. This difference can also be seen in figure 9 where the intra- + inter-molecular distribution functions from the two models are compared with the ND data. This also demonstrates the fact that removing the intramolecular term from the total functions has not introduced any artifacts into the intermolecular functions shown in figure 8. At r-values greater than ∼2.8 Å, figure 9 shows that there are obvious discrepancies between the two simulations and the experiment. While the H1 + CH_3 model seems to be better in reproducing (see inset in figure 8) (i) the peak at ∼5 Å, (ii) the shape of the experimental curve between ∼3 and 5 Å (although the peak along with its right shoulder at ∼3–5 Å is significantly overemphasized) and also (iii) the dropping tail at the low r-end, the APR6 model fails badly in reproducing the experimental function. Nevertheless, neither model gives a quantitative description of the experimental features. Again, reference to figures 3–5 and the relative weights of the three contributions reveal that the differences in the two models arise mainly from the H_O–H and, to a lesser extent, from the C–H_O partials.

The X–X partial, $G_{XX}^{\text{inter}}(r)$, obtained from the NDIS is a weighted sum of the six non-substituted atom–non-substituted atom contributions.

$$G_{XX}^{\text{inter}}(r) = \sum_{X_1 \neq H_O} \sum_{X_2 \neq H_O} W_{X_1X_2} g_{X_1X_2}(r) \qquad \text{where } X_1, X_2 = \text{C, O and H.} \tag{5}$$

Out of the six contributions contained within this function, three of them, H–H (38%), C–H (25%) and H-O (22%), taken together represent 85% of the total. This rdf is thus dominated by contributions from the methyl groups. MD equivalents of this function were constructed from the pdfs as before, and results from both the ND and MD are displayed in figure 10. The

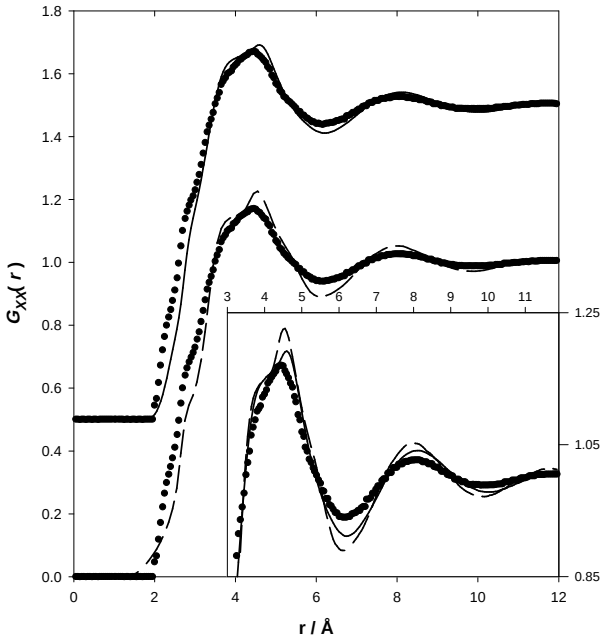

Figure 10. The X–X partial distribution functions obtained from MD simulations using the H1 + CH_3 model (dashed line) and the APR6 model (solid line displaced by +0.5) compared to the partial distribution function obtained experimentally (symbols). The same functions are overlaid on a different scale in the inset.

overall agreement between the two simulations and experiment is satisfactory. The closest distance of approach in the H1 + CH_3 model is seen to be lower than both the experimental distance and the value from the APR6 model. It would appear that the methyl hydrogens, which are specific interaction sites in the APR6 model, cannot come closer together as they can in the case of H1 + CH_3 model potential. Although the oscillations smear out more quickly in ND than in the simulations, the two models reproduce the experimental results equally well at higher distances. This is contrary to the fact that clear differences can be seen in figure 5 between the two models in the contributing H–H, C–H and O–H pdfs. A plausible explanation is that cancellation effects play a role when $G_{XX}^{\text{inter}}(r)$ is computed from a neutron weighted sum of the three contributing terms.

The results from our previous MD simulations carried out using a three-site model [16] showed that the methyl group did not participate in any intermolecular bonding. In the current simulations, addition of three methyl hydrogens as specific interaction sites has not improved the results any further. In this respect, our results do not support the suggestion made by Anwander *et al* [17], that methyl group participates in hydrogen bonds of the form Me–HO::HCH_2–OH and bifurcated H-bonds of the form Me–HO::H_2CH–OH.

5. Conclusions

MD simulations of liquid methanol have been performed with a six-site potential (APR6) derived from *ab initio* quantum chemical calculations [17] for the first time. The presence of inverse cubic terms within the APR6 potential make it impossible to estimate the potential truncation corrections required for accurate calculation of thermodynamic properties such as

enthalpy of vaporization, pressure etc using the DL_POLY. The results of these simulations are compared with experimental structural results [14] obtained by using the H/D substitution technique of neutron diffraction and also with our previously reported [16] simulations using a three-site model (H1 + CH_3). Comparison at the total intermolecular radial distribution function level does not permit us to say that one model is better than the other. However, a comparison of the simulated functions with the corresponding three experimental partial distribution functions, $g_{H_O H_O}(r)$, $G^{\text{inter}}_{XH_O}(r)$ and $G^{\text{inter}}_{XX}(r)$ reveals that although in APR6 the methyl hydrogens are treated as specific interaction sites, the H1 + CH_3 model with the three methyl hydrogens treated as dead load does a better job, though only qualitatively, in reproducing experimental structural features.

Acknowledgments

We are grateful to the EPSRC for continued support of our structural work on a variety of liquids. One of us, LB, is grateful to the University of Abertay-Dundee for the PhD studentship, and ONK acknowledges the Royal Society/NATO for the award of a post-doctoral fellowship.

References

[1] Jorgensen W L 1980 *J. Am. Chem. Soc.* **102** 543
[2] Jorgensen W L 1981 *J. Am. Chem. Soc.* **103** 341
[3] Jorgensen W L 1986 *J. Phys. Chem.* **90** 1273
[4] Palinkas G, Hawlicka E and Heinzinger K 1987 *J. Phys. Chem.* **91** 4334
[5] Hawlicka E, Palinkas G and Heinzinger K 1989 *Chem. Phys. Lett.* **144** 255
[6] Haughney M, Ferrario M and McDonald I R 1987 *J. Phys. Chem.* **91** 4934
[7] Caldwell J W and Kollman P A 1995 *J. Phys. Chem.* **99** 6208
[8] Gao J, Habibollazadeh D and Shao L 1995 *J. Phys. Chem.* **99** 10 400
[9] Jorgensen W L, Maxwell D S and Tirado-Rives J 1996 *J. Am. Chem. Soc.* **118** 11 225
[10] Wang J, Boyd R J and Laaksonen A 1996 *J. Chem. Phys.* **104** 7261
[11] Buck U, Siebers J and Wheatley R J 1998 *J. Chem. Phys.* **108** 20
[12] Svishchev I M and Kusalik P G 1994 *J. Chem. Phys.* **100** 5165
[13] Wright D and El-Shall M S 1996 *J. Chem. Phys.* **105** 11 199
[14] Adya A K, Bianchi L and Wormald C J 1999 *J. Chem. Phys.* submitted
[15] Yamaguchi T 1998 *J. Mol. Liquids* **78** 43
[16] Bianchi L, Kalugin O N, Adya A K and Wormald C J 1999 *Mol. Simul.* submitted
[17] Anwander E H S, Probst M M and Rode B M 1992 *Chem. Phys.* **166** 341
[18] Lees R M and Baker J G 1968 *J. Chem. Phys.* **48** 5299
[19] Ivash E V and Dennison D M 1953 *J. Chem. Phys.* **21** 1804
[20] Schmidt M W *et al* 1993 *J. Comput. Chem.* **14** 1347
[21] McClellan A L 1989 *Tables of Experimental Dipole Moments* (El Cerrito, CA: Rahara Enterprise)
[22] Le Fevre R J W 1953 *Dipole Moments: their Measurement and Application in Chemistry* (New York: Wiley)
[23] Fincham D 1992 *Mol. Simul.* **8** 165
[24] Smith W and Forester T R 1996 *J. Mol. Graph.* **14** 136
[25] Riddick J A, Bunger W B and Sakano T K 1986 *Organic Solvents, Physical Properties and Methods of Purification* 4th edn (New York: Wiley)
[26] De Leeuw S W, Perram J W and Smith E R 1980 *Proc. R. Soc.* A **373** 27
[27] Hurle R L and Woolf L A 1980 *Aust. J. Chem.* **33** 1947
[28] Allen M P and Tildesley D J 1987 *Computer Simulation of Liquids* (Oxford: Clarendon)
[29] Haughney M, Ferrario M and McDonald I R 1986 *Mol. Phys.* **86** 849
[30] Magini M, Paschina G and Paccaluga G 1982 *J. Chem. Phys.* **77** 2051
[31] Tauer K J and Lipscomb W 1952 *Acta Crystallogr.* **5** 606
[32] Narten A H and Habenscuss A 1984 *J. Chem. Phys.* **80** 3387
[33] Wertz D L and Kruh R K 1967 *J. Chem. Phys.* **47** 388
[34] Montague D G, Dore J C and Cummings S 1984 *Mol. Phys.* **53** 1049